

Optical Properties of Lorentz violating Kerr-Sen-like spacetime in the presence of plasma

Sohan Kumar Jha

Chandernagore College, Chandernagore, Hooghly, West Bengal, India

Sahazada Aziz

Ramananda Centenary College, Laulaha-723151, Purulia, West Bengal, India.

Anisur Rahaman*

Hooghly Mohsin College, Chinsurah, Hooghly - 712101, West Bengal, India

(Dated: October 11, 2021)

Abstract

Einstein-bumblebee gravity renders a Kerr-Sen-like black hole solution that contains a Lorentz violating parameter. We study the null geodesics in the background of this Kerr-Sen-like black hole surrounded by a plasma medium using. We investigate the effect of the charge of the black hole, the Lorentz violation parameter and plasma parameter on the photon orbits with the evaluation on the effective potential in the presence of both the Lorentz violation parameter and the plasma parameter. We also study the influence of the Lorentz violation parameter and plasma parameter on the emission of energy from the black due to thermal radiations. Besides we compute the angle of deflection of the massless particles with weak-field approximation in this generalized situation and examine how it varies with the Lorentz violation parameter in presence of plasma.

PACS numbers:

I. INTRODUCTION

After the announcement of the detection of gravitational waves (GWs)[1] by the LIGO and VIRGO observatories, and the captured image of the black hole shadow of a super-massive $M87^*$ black hole by the Event Horizon Telescope based on the very long baseline interferometry [2, 3] the physics of black hole has got renewed interest. A black hole shadow is a two dimensional dark zone in the celestial sphere caused by the strong gravity of the black hole. In the article [4], Synge studied the shadow of the Schwarzschild black hole, which was then termed as the escape cones of light. The radius of the shadow of the black hole was calculated in terms of the mass of the black hole and the radial coordinate where the observer is located. In general, the shadow for a non-rotating black hole is a standard circle, whereas it is known that the shadow of a rotating black hole is not a circular disk. The different features of the black hole have been widely investigated for various gravity backgrounds adopting an almost similar approach based on classical dynamics [5–21].

In general relativity, light is attributed to the null geodesic of the spacetime metric and the in-medium effect though negligible for most of the frequency ranges, for the radio frequency range however, it shows a significant effect. In this context, it is worth mentioning that the impact of the Solar corona on the time of travel and on the deflection angle of radio signals that come close to the Sun. Since the 1960s, this influence has been routinely observed. In this case, one may assume that the medium is a non-magnetized pressureless plasma and for the gravitational field, the linearized theory is sufficient. The relevant theoretical development has been made by Muhleman et al. in the articles [22, 23]. With the available information, the shadow of black holes in presence of plasma has become an interesting field of research for physicists since there is a good reason for considering that the black holes and the other compact objects are surrounded by plasma. So naturally, interest grows to investigate whether the presence of plasma leads to any observation effect on the radio signal and several investigations have been carried out in that direction [24–35].

The physics of black holes is crucially linked with the Planck energy scale where gravity is sufficiently strong and a classical field theory of curved spacetime is not adequate to capture the finer details of the Planck scale. It needs quantization of gravity which is not well developed. However, it is reasonable to accept that in that scale nature of the spacetime is discrete. Lorentz symmetry being a continuous symmetry, would not be tenable in discrete

*Electronic address: anisur.rahman@saha.ac.in (Corresponding Author)

spacetime. Moreover, according to string theory, Lorentz invariance should not be an exact principle at all energy scales [36–39]. If Lorentz violation is considered to be a probe for the foundation of theoretical physics suitable model is therefore needed which contains Lorentz violation adopted from standard physical principle. The known two well-developed and successful theories that describe our Universe are General relativity and the standard model of particle physics. These theories are build up obeying Lorentz invariance and these two theories are applicable in two different energy scales. The standard model describes the three fundamental interactions at the quantum level whereas general relativity describes the gravitational interaction at the classical level. A single complete theory requires the unification of these two. However, there is a strong obstacle in the way of unification since gravity can not be quantized in a straightforward manner. So even with huge efforts from different fronts, a successful unified theory has not been developed. To unify them at very high energy scales, one builds an effective field theory termed standard model extension(SME), that couples the SM to GR, that involves extra items containing information about the Lorentz violation(LV) happening at the Plank scale [40–42]. The simplest case is described by a single vector bumblebee field, with a nonzero vacuum expectation value and the spontaneous LV triggered by a smooth quadratic potential. Bumblebee gravitational model was first studied by Kostelecky and Samuel in [36–38] as a specific pattern for unprompted Lorentz violation. Therefore, Lorentz violation may be considered as a good probe to the foundation physics.

In this context, the study of Lorentz violation effect on the shadow of a black hole in presence of Plasma would be of interest. There are several recent investigations to study the deformation of black hole shadow due to the Lorentz violation effect [43, 44]. In these studies, the in-medium (plasma) effect has not been considered so far. Therefore, the study of the deformation of the shadow of the black hole connected with Kerr-sen-like spacetime, the emission of energy from this black hole due to radiation, and the weak lensing in the presence of plasma would be an interesting extension. The black hole associated with Kerr-sen-like spacetime [43] contains a Lorentz violating parameter like Schwarzschild-like and Kerr-like spacetime [44, 45]. This Kerr-sen-like spacetime will enable us to study the Lorentz violation effect in presence of Plasma.

So in this paper, we will consider Einstein gravity coupled to the bumblebee fields, to get some suppressed effects emerging from the underlying unified quantum gravity theory, on our low energy scale. Recently, Casana et al. [45] gave an exact Schwarzschild-like the solution in this bumblebee gravity model and considered its some classical tests. The rotating black hole solutions are the most relational subsets for astrophysics. In [44], Ding et al found an exact Kerr-like solution by solving Einstein-bumblebee gravitational field equations and studied its black hole shadow. Then in the article [46] study the weak gravitational deflection angle of relativistic massive particles by this Kerr-like black hole. We in [43], extended this Kerr-like solution to the Kerr-sen case.

The article is organized as follows. In Sec. II we study the null geodesics around the charged rotating Kerr-sen-like black hole in the presence of plasma. In Sec. III, we study the shadow corresponding to this charged rotating black hole and how the shadow gets deformed with the variation of charge, Lorentz violating parameter, and the plasma parameter has been studied thoroughly. Sec IV is devoted to the study of emission of energy due to thermal radiation for this black hole and to the study of the effect of Lorentz violating parameter, and the plasma parameter on it. In Sec. V we study the deflection angle of light with weak-field approximation in this Lorentz violating spacetime background in the presence of plasma. The final Sec. VI contains brief summary and discussion

II. NULL GEODESICS AROUND THE CHARGED ROTATING KERR-SEN-LIKE BLACK HOLE IN THE PRESENCE OF PLASMA

It is known that Einstein-Bumblebee gravity provides Schwarzschild-like, Kerr-like as well as Kerr-Sen-like black-hole metric. In Boyer-Lindquist coordinates, the Kerr-Sen-like charged rotating metric results out from the Einstein-bumblebee gravity that reads [43]

$$ds^2 = - \left(1 - \frac{2Mr}{\rho^2} \right) dt^2 - \frac{4Mr a \sqrt{1 + \ell} \sin^2 \theta}{\rho^2} dt d\varphi + \frac{\rho^2}{\Delta} dr^2 + \rho^2 d\theta^2 + \frac{A \sin^2 \theta}{\rho^2} d\varphi^2. \quad (1)$$

where

$$\rho^2 = r(r + b) + a^2(1 + \ell), \Delta = \frac{r(r + b) - 2Mr}{1 + \ell} + a^2, A = [r(r + b) + (1 + \ell)a^2]^2 - \Delta(1 + \ell)^2 a^2 \sin^2 \theta. \quad (2)$$

The parameter a and b are related with angular momentum and charge of the black hole by the relations $J = \frac{M}{a}$ the $Q = \sqrt{bM}$ respectively. Here M , Q , and J respectively refer to the mass, charge, and angular momentum. The expression of ρ and Δ contain the parameter ℓ that represents the Lorentz violation parameter which is associated

with spontaneous violation of symmetry of the vacuum of the bumblebee field. If $\ell \rightarrow 0$ it recovers the usual Kerr-Sen metric and for $a \rightarrow 0$, and $b \rightarrow 0$ the metric turns into

$$ds^2 = - \left(1 - \frac{2M}{r}\right) dt^2 + \frac{1 + \ell}{1 - 2M/r} dr^2 + r^2 d\theta^2 + r^2 \sin^2 \theta d\varphi^2, \quad (3)$$

which is the Schwarzschild-like solution for the Einstein-bumblebee gravity [44, 45].

We consider a static inhomogeneous plasma in the gravitational field with a refractive index n . The expression of refractive index n as formulated by Synge [47], in terms of dynamical variables reads

$$n^2 = 1 + \frac{p_\mu p^\mu}{(p_\nu u^\nu)^2}. \quad (4)$$

where p_μ and u^ν are four-momentum and four-velocity of the massless particle. Let us now start with the Hamiltonian for massless particles like photon:

$$H(x^\mu, p_\mu) = \frac{1}{2} \left[g^{\mu\nu} p_\mu p_\nu - (n^2 - 1) (p_0 \sqrt{-g^{00}})^2 \right]. \quad (5)$$

The standard definitions $x^\mu = \partial H / \partial p_\mu$ and $\dot{p}_\mu = \partial H / \partial x^\mu$ lead us to write down the equations of motion for photon in the plasma medium as follows

$$\rho^2 \frac{dr}{d\lambda} = \pm \sqrt{R}, \quad \rho^2 \frac{d\theta}{d\lambda} = \pm \sqrt{\Theta}, \quad (6)$$

$$(1 + \ell) \Delta \rho^2 \frac{dt}{d\lambda} = An^2 - 2\sqrt{1 + \ell} Mra\xi, \quad (7)$$

$$(1 + \ell) \Delta \rho^2 \frac{d\phi}{d\lambda} = 2Mra\sqrt{1 + \ell} + \frac{\xi}{\sin^2 \theta} (\rho^2 - 2Mr), \quad (8)$$

where λ is the affine parameter, and

$$\begin{aligned} R(r) &= \left[\frac{r(r+b) + (1+\ell)a^2}{\sqrt{1+\ell}} - a\xi \right]^2 - \Delta \left[\eta + (\xi - \sqrt{1+\ell}a)^2 \right] + (n^2 - 1) \frac{[r(r+b) + a^2(1+\ell)]^2}{1+\ell}, \\ \Theta(\theta) &= \eta + (1+\ell)a^2 \cos^2 \theta - \xi^2 \cot^2 \theta - (n^2 - 1) a^2 (1+\ell) \sin^2 \theta. \end{aligned} \quad (9)$$

In the equation (9), we introduce two conserved parameters ξ and η as usual which are defined by

$$\xi = \frac{L_z}{E}, \quad \eta = \frac{\mathcal{Q}}{E^2}, \quad (10)$$

where E , L_z , and \mathcal{Q} are the energy, the axial component of the angular momentum and *Carter constant*, respectively.

We introduce a static inhomogeneous plasma with a refraction index n , which depends on the space location \mathbf{x} and the photon frequency ω [33]. In terms of ω , the square of the refractive index n is defined by

$$n^2 = 1 - \frac{\omega_e^2}{\omega^2}. \quad (11)$$

where, ω and ω_e , are respectively the frequency of photon and electron-plasma frequency. In the general theory of relativity, the redshift scenario entails that frequency of photons depends on the spatial coordinates due to the presence of the gravitational field. Besides the electron-plasma frequency has the expression [48]

$$\omega_e^2 = \frac{4\pi e^2 N(r)}{m}, \quad (12)$$

where, $N(r)$ is the concentration of electron in the inhomogeneous plasma, m and e are the mass and the charge of the electron respectively. We now consider a radial power-law density as

$$N(r) = \frac{N_0 r_0}{r^h}, \quad (13)$$

where N_0 is the density number at the radial position of the inner edge of plasma environment r_0 . So, we have

$$\omega_e^2 = \frac{4\pi e^2 N_0 r_0}{m r^h}, \quad (14)$$

where $h \geq 0$. Here we consider $h = 1$ as it has been considered in the article [49]. So that we have

$$n = \sqrt{1 - \frac{k}{r}}. \quad (15)$$

With this specific form of refractive index, we study various aspects of photon geodesics with the spacetime metric given in Eq. (1). The radial equation of motion has the known form

$$\left(\rho^2 \frac{dr}{d\lambda}\right)^2 + V_{eff} = 0. \quad (16)$$

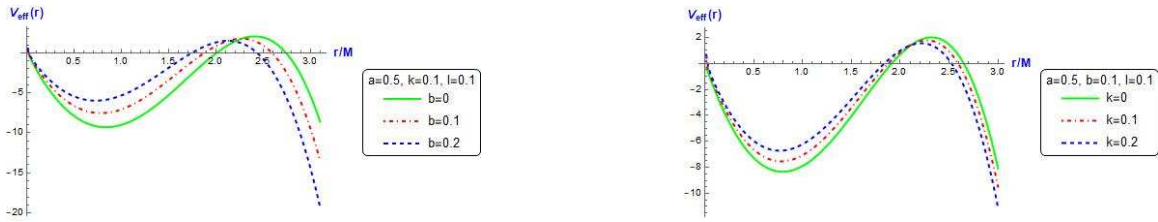
The effective potential V_{eff} in this situation reads

$$V_{eff} = -\left[\frac{r(r+b) + (1+\ell)a^2}{\sqrt{1+\ell}} - a\xi\right]^2 + \Delta \left[\eta + (\xi - \sqrt{1+\ell}a)^2\right] - (n^2 - 1) \frac{[r(r+b) + a^2(1+\ell)]^2}{1+\ell} \quad (17)$$

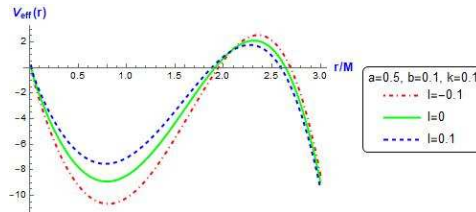
Note that it contains both the factor ℓ and k . The shape of the orbit crucially depends on the nature of the effective potential. So it is natural that the orbit will have crucial dependence on both the factor ℓ and k in this situation. The unstable spherical orbit on the equatorial plane will be obtained if the following conditions are met:

$$\theta = \frac{\pi}{2}, R(r) = 0, \frac{dR}{dr} = 0, \frac{d^2R}{dr^2} > 0, \eta = 0. \quad (18)$$

We plot the V_{eff} versus r/M with $\xi = \xi_c + 0.2$ where ξ_c is the value of ξ for equatorial spherical unstable direct orbit. For all the calculations and plots in this paper, we have taken $M = 1$. In Fig.1 we find that the turning point moves to the left for the increase of the value of b for a fixed k and ℓ are fixed. It also shifts to the left with the increasing value of k when b and ℓ remain fixed. For the positive value of the Lorentz violating parameter ℓ it also shifts to the left however for the negative value of the ℓ it gets shifted towards the right like the case when plasma was absent [43]. In Fig.2, if we observe the plot of the critical radius we find that r_c decreases with the increase of the value of b for fixed k and ℓ and it increases with the increase of the value of k when b and ℓ remain fixed. However for $l > 0$ the critical radius r_c although decrease for $l < 0$ it increases.



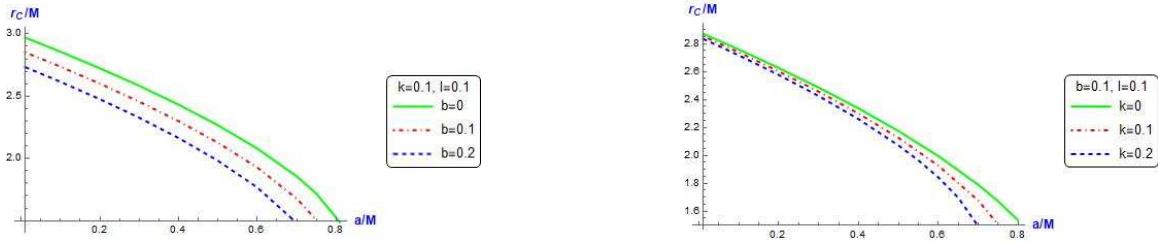
(a) Effective potential for various values of b with $a/M = .5, l = .1, k = .1$ and $\theta = \pi/2$ (b) Effective potential for various values of k with $a/M = .5, l = .1, b = .1$ and $\theta = \pi/2$



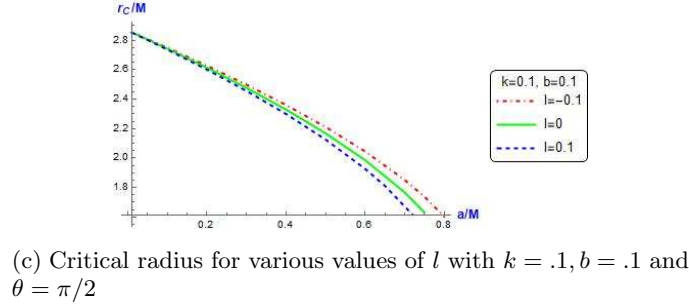
(c) Effective potential for various values of l with $a/M = .5, k = .1, b = .1$ and $\theta = \pi/2$

FIG. 1: Plots of effective potential for various scenarios

We also plot critical radius versus a keeping $\theta = \frac{\pi}{2}$. To plot it we consider variations of parameters b, k and ℓ involved in our our purposed model.



(a) Critical radius for various values of b with $l = .1, k = .1$ and $\theta = \pi/2$ and (b) Critical radius for various values of k with $l = .1, b = .1$ and $\theta = \pi/2$



(c) Critical radius for various values of l with $k = .1, b = .1$ and $\theta = \pi/2$

FIG. 2: Plots of Critical radius for various scenarios

For more generic spherical orbits where $\theta \neq \pi/2$ and $\eta \neq 0$, the conserved quantities ξ_s and η_s for $r = r_s$, is given by the simultaneous solutions of

$$R = 0, \frac{dR}{dr} = 0 \quad (19)$$

III. BLACK HOLE SHADOW

To describe the nature of the shadow that an observers see in the sky, the following two celestial coordinates will be helpful

$$\alpha(\xi, \eta; \theta) = -\frac{\xi_s \csc \theta}{n},$$

$$\beta(\xi, \eta; \theta) = \frac{\sqrt{\eta + (1 + \ell)a^2 \cos^2 \theta - \xi^2 \cot^2 \theta - (n^2 - 1)a^2(1 + \ell) \sin^2 \theta}}{n} \quad (20)$$

Let us now proceed to see the shape and size of the shadows. The nature of the shadow will depend on the various parameters. So we sketch the black hole shadow for various possible causes. In Fig. 3, the sketch shows that with the increase of the value of b the size of the shadow decrease and the left end of the shadow moves a little to the right when k and ℓ remain fixed. The deformation of the shadow is not so great. Fig. 4 shows the change of shape of the shadow with a variation of the plasma parameter k keeping b and ℓ fixed. The figure shows that the size of the shadow increases with the increase of the value of k . Here deformation of the shape of the shadow can not be found pictorially however mathematically very little deviation is observed. Please see TABLE.1. Fig 5. shows that for a negative value of ℓ the left end of the shadow shifts towards the left and for the positive value of ℓ it shifts towards the right. Deformation of the shape of the shadow is prominent.

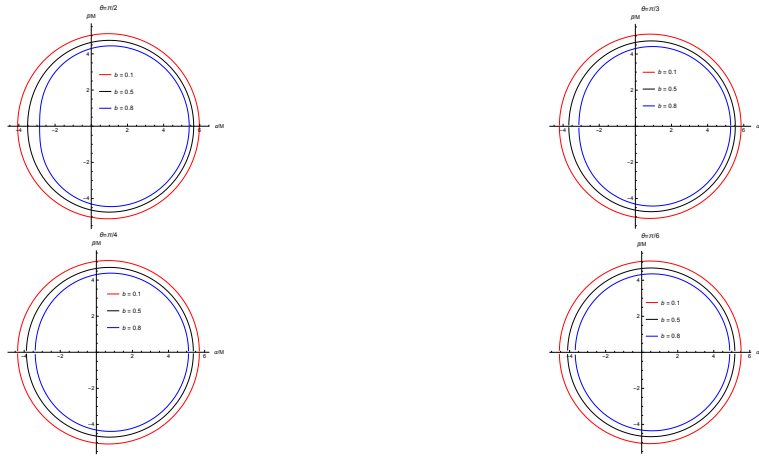


FIG. 3: Shadows for different values of b and θ with $a = .4, k = .2$ and $l = .2$

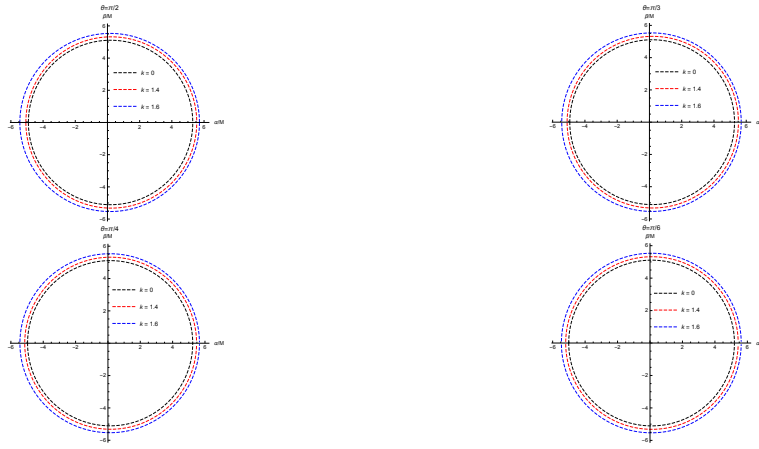


FIG. 4: Shadows for different values of k and θ with $a = .1, b = .1$ and $l = -.1$

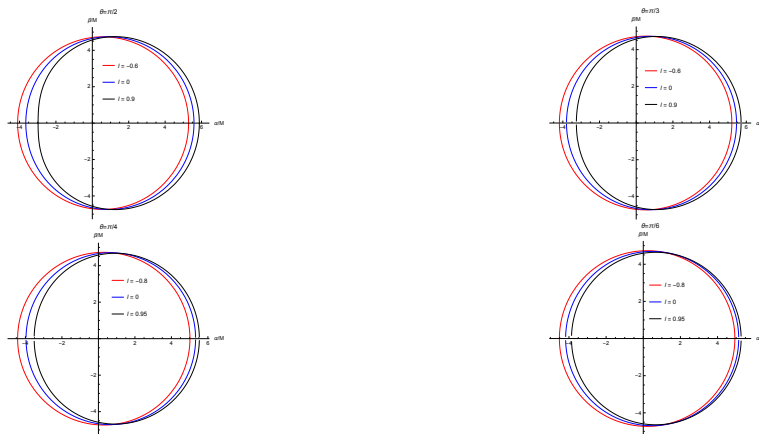


FIG. 5: Shodws for different values of l and θ with $a = .4, b = .5$ and $k = .2$

Using the parameters which are introduced by Hioki and Maeda in [5], we analyze deviation from the circular form of the shadow (δ_s) and the size (R_s) of the shadow image of the black hole.

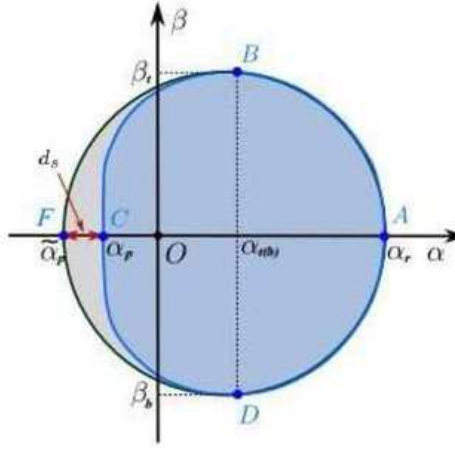


FIG. 6: The black hole shadow and reference circle. d_s is the distance between the left point of the shadow and the reference circle [50]

For calculating these parameters, we consider five points (α_t, β_t) , (α_b, β_b) , $(\alpha_r, 0)$, $(\alpha_p, 0)$ and $(\bar{\alpha}_p, 0)$ which are top, bottom, rightmost, leftmost of the shadow and leftmost of the reference circle respectively. From simply geometry we have

$$R_s = \frac{(\alpha_t - \alpha_r)^2 + \beta_t^2}{2(-\alpha_t + \alpha_r)}, \quad (21)$$

and

$$\delta_s = \frac{(-\bar{\alpha}_p + \alpha_p)}{R_s}. \quad (22)$$

For all subsequent plots we have taken $\theta = \pi/2$

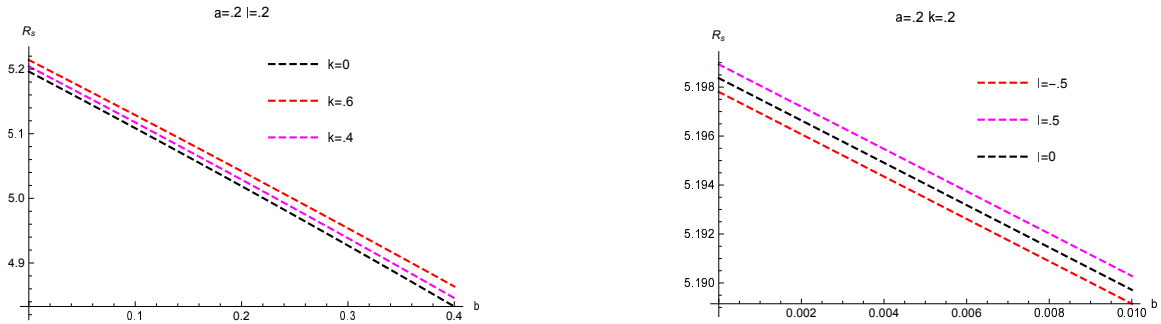


FIG. 7: The left one gives the variation of R_s with b for different values of k with $a = .2, l = .2$, and the right one gives the variation of R_s with b for different values of l with $a = .2, k = .2$

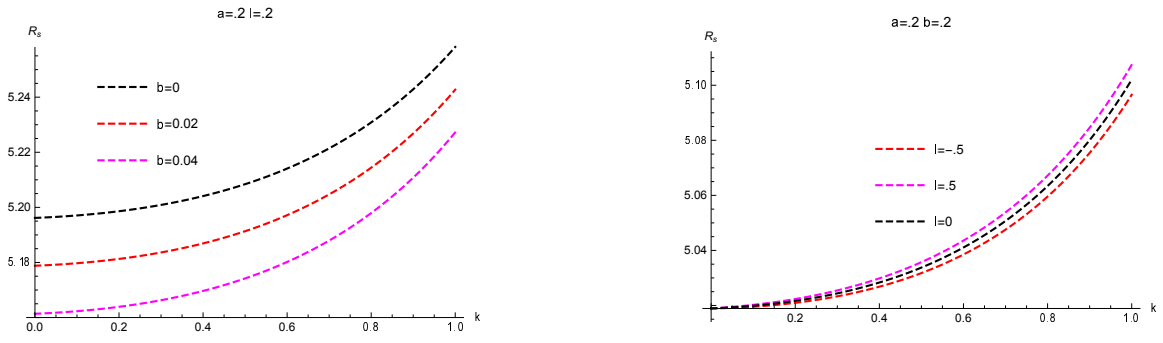


FIG. 8: The left one gives the variation of R_s with k for different values of b with $a = .2, l = .2$ and the right one gives the variation of R_s with k for different values of l with $a = .2, b = .2$

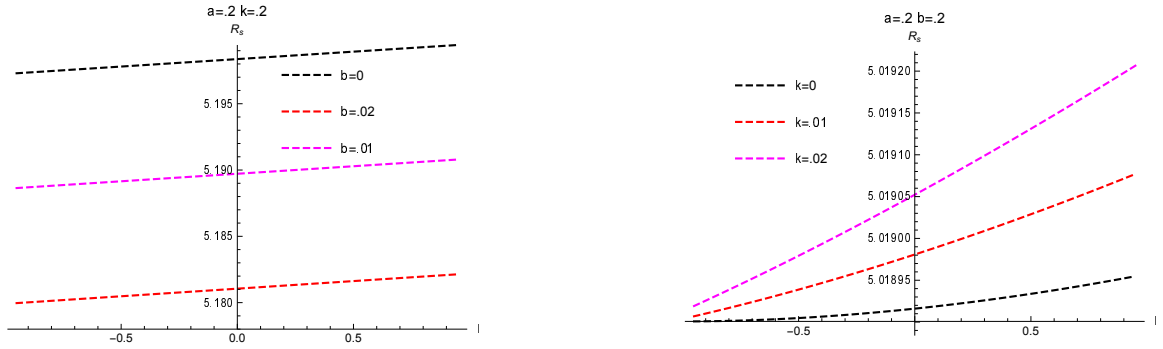


FIG. 9: The left one gives the variation of R_s with l for different values of b with $a = .2, k = .2$ and the right one gives the variation of R_s with l for different values of k with $a = .2, b = .2$

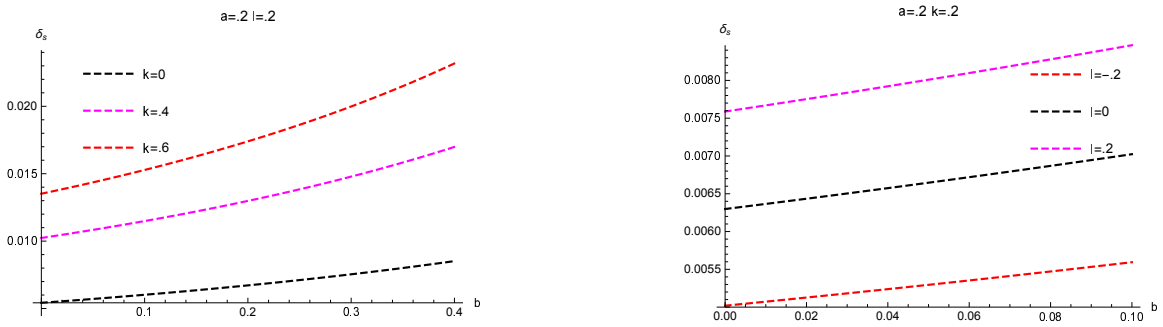


FIG. 10: The left one gives the variation of δ_s with b for different values of k with $a = .2, l = .2$ and the right one gives the variation of δ_s with b for different values of l with $a = .2, k = .2$

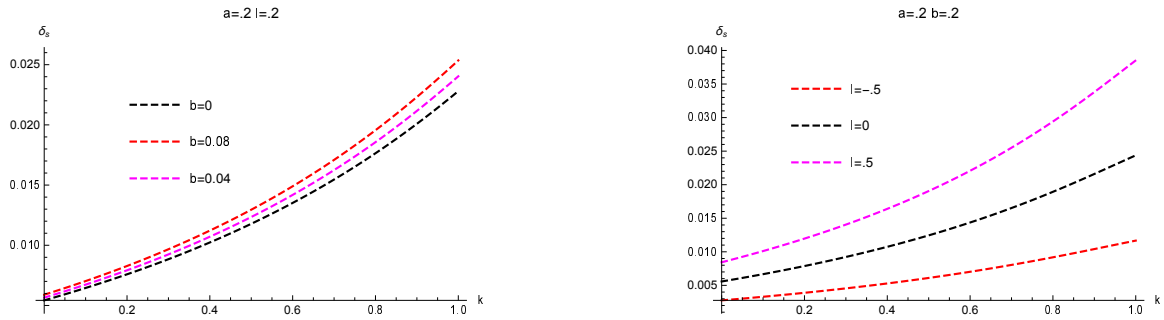


FIG. 11: The left one gives the variation of δ_s with k for different values of b with $a = .2, l = .2$ and the right one gives the variation of δ_s with k for different values of l with $a = .2, b = .2$

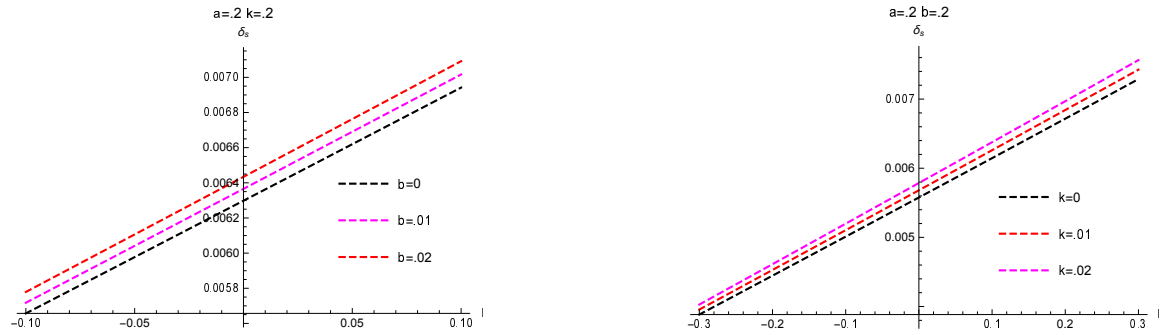


FIG. 12: The left one gives the variation of δ_s with l for different values of b with $a = .2, k = .2$ and the right one gives the variation of δ_s with l for different values of k with $a = .2, b = .2$

Here we have give in a tabular form the deviation of the image δ_s of the Kerr-sen-like black hole for set of values of $k \equiv \{0, .01, .02\}$ corresponding to the set of values of $l \equiv \{-.2, 0, .2\}$ with $a = b = 0.2$ and $\theta = \frac{\pi}{2}$.

TABLE I: Deviation δ_s of Kerr-sen-like BH with $a = b = 0.2$

	$l = -.2$	$l = 0$	$l = .2$
$k = 0$	0.00444613	0.00557717	0.00671623
$k = .01$	0.00452873	0.00568118	0.00684196
$k = .02$	0.00461217	0.00578625	0.00696899

IV. ENERGY EMISSION RATE

It is known that the black holes emit radiation and consequently the mass of the black hole decrease and the process continues until it collapses down completely [51]. For various black holes, this emission rate has been studied. In [43], we have studied the energy emission rate for Kerr-sen-like black holes and studied the consequences of Lorentz violation effect ℓ on it. Here we would like to study the energy emission in presence of plasma. The energy emission rate of radiation with the frequency ω is given by

$$\frac{d^2E}{d\omega dt} = \frac{2\pi^3 R_s^2}{e^{(\frac{\omega}{T})} - 1} \omega^3 \quad (23)$$

where ω is the frequency and T is the Hawking temperature given by [43]

$$T = \frac{\sqrt{(2M - b)^2 - 4a^2(1 + l)}}{4\pi M \sqrt{1 + l} \left(2M - b + \sqrt{(2M - b)^2 - 4a^2(1 + l)} \right)} \quad (24)$$

The energy emission rate is directly proportional to the surface area of the black hole which may be considered to be approximately equal to the surface area of the shadow $S \approx \pi R_s^2$. Computing R_s using the expression (21) and using (24) we can calculate the rate of emission of radiation which enables us to plot energy emission versus frequency of radiation curve. In Fig. 13 we have studied how the energy emission rate will behave for the variation of the parameter b , ℓ , and k . It is observed that the rate of emission is higher for smatter values of b . However, the reverse is the case when k increases. It is evident from the spectrum that in the absence of plasma the minimum energy will be released from the black hole which indeed agrees with the Kerr-Newman black hole [35]. The variation of ell shows that for negative ℓ there is an enhancement of emission whereas for increasing positive ℓ reduction of emission of radiation.

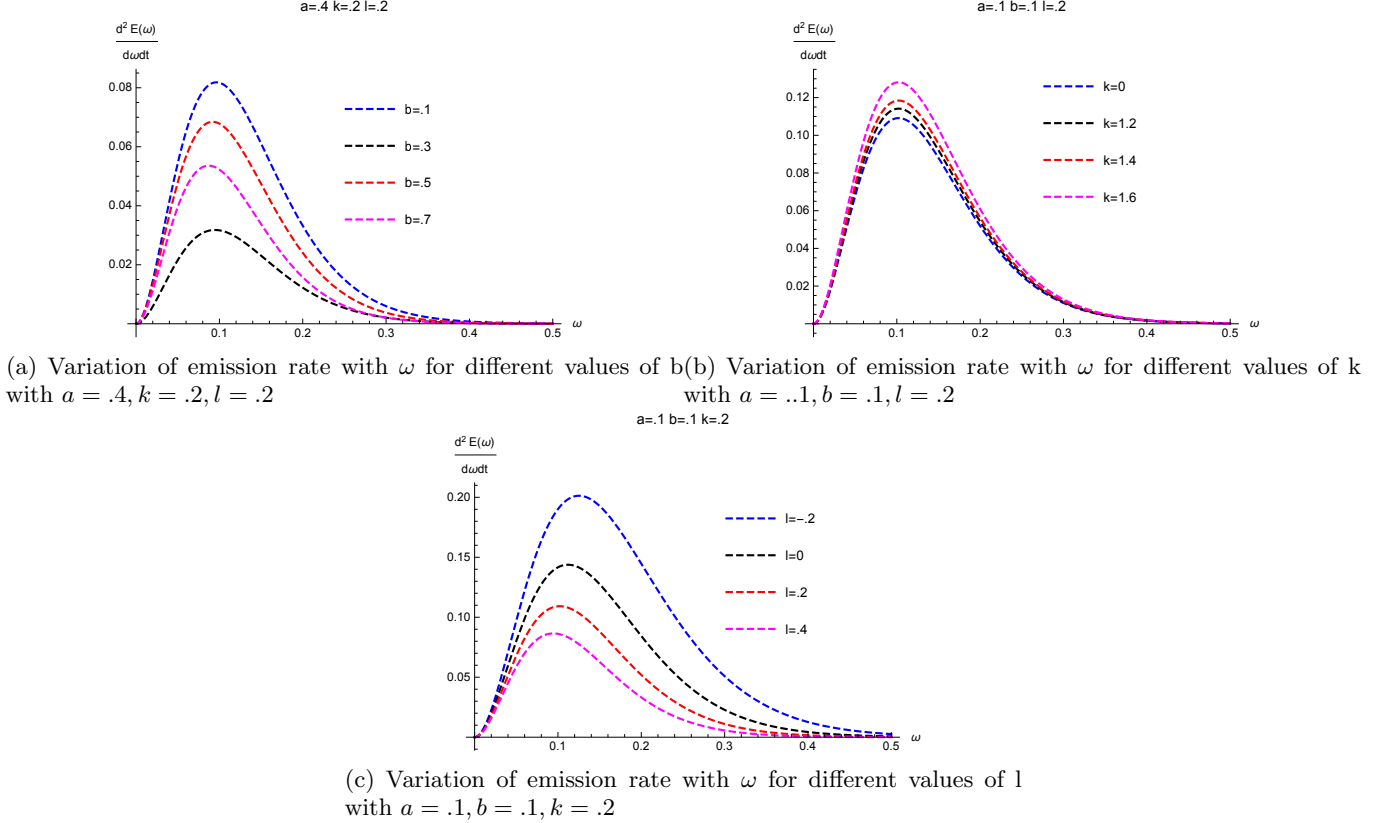


FIG. 13: Variation of emission rate with ω for different situations

V. DEFLECTION ANGLE OF LIGHT IN WEAK FIELD IN THE PRESENCE OF PLASMA

The deflection of light or lensing in presence of plasma for different spacetime backgrounds has been studied in the earlier literature [52–54]. The extension of it for this Kerr-Sen-like black hole is worth investigation. There is a Lorentz violating parameter ℓ . So from our study, the combined effect of the presence of plasma and Lorentz violation on the deflection of light can be estimated. To study it weak field approximation will be useful. This approximation is given by the expression

$$g_{\mu\nu} = \eta_{\mu\nu} + h_{\mu\nu}, \quad (25)$$

where $\eta_{\mu\nu}$ is the Minkowski metric and $h_{\mu\nu}$ refers the perturbation metric over $\eta_{\mu\nu}$, respectively. The Minkowski metric $\eta_{\mu\nu} = \text{diag}(-1, 1, 1, 1)$ and $h_{\mu\nu}$ has the the following properties under weak field approximation

$$h_{\mu\nu} \ll 1, \quad h_{\mu\nu} \rightarrow 0 \quad \text{under} \quad x^i \rightarrow \infty$$

$$g^{\mu\nu} = \eta^{\mu\nu} - h^{\mu\nu}, \quad h^{\mu\nu} = h_{\mu\nu} \quad (26)$$

Considering the weak plasma strength the angle of deflection of photon propagating along z direction under weak field the approximation is given by [55]

$$\hat{\alpha}_k = \frac{1}{2} \int_{-\infty}^{\infty} \left(h_{33} + \frac{h_{00}\omega^2 - K_e N}{\omega^2 - \omega_e^2} \right) dz. \quad (27)$$

where $K_e = \frac{4\pi e^2}{m}$. For large r , the black hole metric approximately be written down in the form

$$ds^2 = ds_0^2 + \left(\frac{2M}{r} - \frac{2Mb}{r^2} \right) dt^2 + (1+l) \left(\frac{2M}{r} - \frac{2Mb}{r^2} \right) dr^2 \quad (28)$$

where

$$ds_0^2 = -dt^2 + (1+l) dr^2 + r^2 (d\theta^2 + \sin^2 \theta d\phi^2) \quad (29)$$

The components $h_{\alpha\beta}$ in in the Cartesian coordinates have the following expression

$$\begin{aligned} h_{00} &= \left(\frac{R_g}{r} - \frac{2Mb}{r^2} \right) \\ h_{ik} &= (1+l) \left(\frac{R_g}{r} - \frac{2Mb}{r^2} \right) n_i n_k \\ h_{33} &= (1+l) \left(\frac{R_g}{r} - \frac{2Mb}{r^2} \right) \cos^2 \chi \end{aligned}$$

where $R_g = 2M$ and χ is the polar angle between 3-vector and z -axis. Using the above expressions in (27), the light deflection angle for a black hole sitting in plasma medium [52–54, 56] is given by

$$\hat{\alpha}_p = \frac{1}{2} \int_{-\infty}^{\infty} \frac{p}{r} \left(\frac{dh_{33}}{dr} + \frac{\omega^2}{\omega^2 - \omega_e^2} \frac{dh_{00}}{dr} - \frac{K_e}{\omega^2 - \omega_e^2} \frac{dN}{dr} \right) dz \quad (30)$$

where $p^2 = x_1^2 + x_2^2$ refers the impact parameter, and x_1 and x_2 are the coordinates on the plane orthogonal to the z axis and $r = \sqrt{p^2 + z^2}$. We have the relation for the frequency of photon

$$\omega^2 = \frac{\omega_\infty^2}{\left(1 - \frac{R_g}{r} + \frac{2Mb}{r^2} \right)}. \quad (31)$$

Here, ω_∞ is the asymptotic value of photon frequency. After expanding in series on the powers of $\frac{1}{r}$ we can have the approximation

$$\left(1 - \frac{\omega_e^2}{\omega^2} \right)^{-1} \simeq 1 + \frac{4\pi e^2 N_0 r_0}{m\omega_\infty^2 r} - \frac{4\pi e^2 N_0 r_0 R_g}{m\omega_\infty^2 r^2} \quad (32)$$

Using this approximation one can find the deflection angle $\hat{\alpha}_p$ of the light around a black hole in presence of plasma in a straightforward manner

$$\hat{\alpha}_p = (1+l) \frac{2R_g}{p} + \frac{2R_g}{p} \left(1 + \frac{\pi^2 e^2 N_0 r_0}{m\omega_\infty^2 p} - \frac{4\pi e^2 N_0 r_0 R_g}{m\omega_\infty^2 p^2} \right) \quad (33)$$

$$- \frac{2Mb}{4p^2} \left(3\pi + \frac{4\pi e^2 N_0 r_0}{m\omega_\infty^2 p} \left(8 - \frac{3\pi R_g}{p} \right) \right). \quad (34)$$

We get $\hat{\alpha}_p = (1+l) \frac{2R_g}{p}$ in the absence of charge and plasma for the Schwarzschild black hole. The dependence of the angle of deflection $\hat{\alpha}_p$ on the impact parameter, p for various charge and plasma parameters are demonstrated in the figure below. In the left panel, it is found that as the value of b increases the angle of deflection decreases and it is seen that $\hat{\alpha}_p$ is maximum when $b = 0$. We also observe that the deflection angle $\hat{\alpha}_p$ increases with the increase in the plasma parameter (right panel). We also notice that the deviation of photons is smaller when the plasma factor is removed from the black hole background. It is also observed that the deflection angle increases with an increase in the value of the Lorentz violating parameter ℓ .

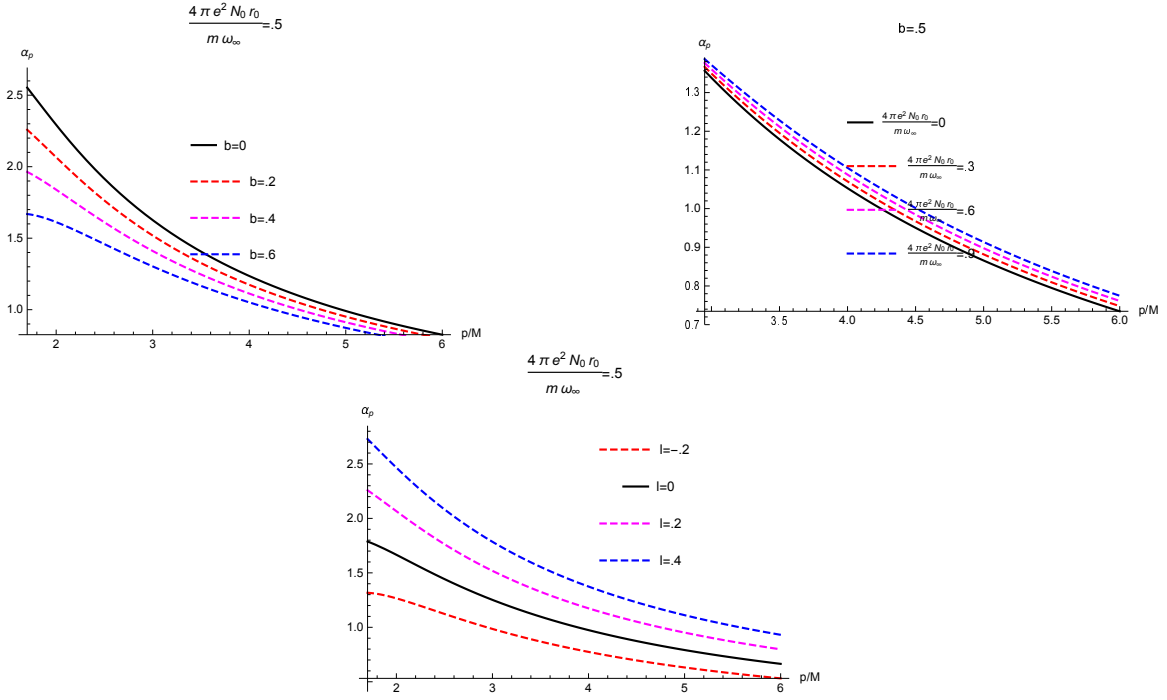


FIG. 14: The left one gives the variation of $\hat{\alpha}_p$ with p/M for different values of b with $\frac{4\pi e^2 N_0 r_0}{m\omega_\infty^2} = .5, l = .2$, the lower one gives the variation of $\hat{\alpha}_p$ with p/M for different values of l with $\frac{4\pi e^2 N_0 r_0}{m\omega_\infty^2} = .5, b = .2$ and The right one gives the variation of $\hat{\alpha}_p$ with p/M for different values of $\frac{4\pi e^2 N_0 r_0}{m\omega_\infty^2}$ with $b = .5, l = .2$

VI. CONCLUSION

We have considered the Kerr-Sen-like black hole which is a solution of Einstein-bumblebee gravity. It contains a Lorentz violating parameter ℓ . We study the propagation of light in a non-magnetized pressureless plasma on this Kerr-Sen-like spacetime. Here we have considered that the plasma as a medium with dispersive properties given by a frequency-dependent index of refraction. The gravitational field is determined by the mass, the spin, and the bumblebee parameter. Gravitational field due to plasma is neglected here. We study how the nature of shadows will be affected by the Lorentz-violating effect associated with the bumblebee field in the pressure-less nonmagnetic plasma. We have also studied the energy emission scenario and the weak field lensing in the Kerr-Sen-like spacetime due to Einstein-bumblebee gravity background when it is filled with a plasma medium. The results for Kerr and Kerr-like as well as Schwarzschild black holes can be obtained from this result with the suitable limit. We have investigated in details the impact of the charge ($Q^2 \propto b$), plasma parameter (k), and Lorentz-violating bumblebee parameter (ℓ) on the structure of shadow, on the lensing effect of light, and on the energy emission scenario due to black hole radiation. It is observed that the shadow size viewed by a distant observer reduces with an increase of Q and the size of the shadow appears to be larger with the increase of plasma in presence of a bumblebee field too. The bumblebee field maintains its action of deforming the shadow in presence of plasma too. Since the energy liberated from the black hole depends on the area of the shadow, therefore, rate of energy emission from the black hole is higher when the black hole is surrounded by a plasma. As far as the angle of deflection is concerned, the photons are observed to experience an increase in the deviation as the plasma factor increases. While on the other hand, the angle of deflection sufficiently reduces when the amount of charge parameter rises. It is also observed that the deflection angle increases with an increase in the value of the Lorentz violating parameter ℓ . Sufficiently negative ℓ may cease the lensing effect too!

[1] B. P. Abbott et al, Phys. Rev. Lett. 116, 061102 (2016).

- [2] K. Akiyama and et al., 'First *M87* Event Horizon Telescope Results. VI. The Shadow and Mass of the Central Black Hole', *Ap. J.* 875 44 (2019).
- [3] K. Akiyama and et al., 'First *M87* Event Horizon Telescope Results. I. The Shadow of the Supermassive Black Hole', *Ap. J.* 875 17 (2019).
- [4] J. L. Synge: *Mon. Not. R. Astron. Soc.* 131 463 (1966).
- [5] K. Hioki and K. I. Maeda, *Phys. Rev. D* 80, 024042 (2009)
- [6] L. Amarilla, E. F. Eiroa, and G. Giribet: *Phys. Rev. D.* 81 124045 (2010).
- [7] F. Atamurotov, B. Ahmedov, and A. Abdujabbarov: *Phys. Rev. D.* 88 064004 (2013)
- [8] S. W. Wei and Y. X. Liu, *J. Cosmol. Astropart. Phys.* 11 (2013) 063.
- [9] A. Abdujabbarov, F. Atamurotov, Y. Kucukakca, B. Ahmedov, U. Camci, , *Astrophys. Space Sci.* 344 429. (2013)
- [10] F. Atamurotov, A. Abdujabbarov, and B. Ahmedov, *Astrophys. Space Sci.* 348 179 (2013)
- [11] U. Papnoi, F. Atamurotov, S. G. Ghosh, and B. Ahmedov: *Phys. Rev. D.* 90 024073 (2014)
- [12] A. Grenzebach, V. Perlick, and C. I. Nammerzahl, *Phys. Rev. D.* 89 124004 (2014)
- [13] Z. Li and C. Bambi, *Journal of Cosmology and Astroparticle Physics* 2014 041 (2014).
- [14] M. Ghasemi-Nodehi, Z. Li, and C. Bambi, *Eur. Phys. J. C.* 75 (2015)
- [15] A. Abdujabbarov, M. Amir, B. Ahmedov, and S. G. Ghosh, *Phys. Rev. D.* 93 104004 (2016)
- [16] F. Atamurotov, S. G. Ghosh, B. Ahmedov: *Eur. Phys. J. C.* 76 (2016)
- [17] G. S. Bisnovaty-Kogan and O. Y. Tsupko: *Phys. Rev. D.* 98 084020 (2018)
- [18] R. Kumar, S. G. Ghosh, A. Wang, *Phys. Rev. D.* 100 124024 (2019)
- [19] S.W. Wei, Y.X. Liu, R. B. Mann: *Phys. Rev. D.* 99 041303 (2019)
- [20] M. Khodadi, A. Allahyari, S. Vagnozzi, D. F. Mota: *JCAP* 2009 026 (2020)
- [21] M. Khodadi, A. Allahyari, S. Vagnozzi, D. F. Mota: *JCAP* 2002 003 (2020)
- [22] D. O. Muhleman, I. D. Johnston, *Phys. Rev. Lett.* 17, 455 (1966)
- [23] D. O. Muhleman, R. D. Ekers, E. D. Fomalont, *Phys. Rev. Lett.* 24, 1377 (1970)
- [24] G. S. Bisnovaty-Kogan and O. Y. Tsupko: *Mon. Not. R. Astron. Soc.* 404 1790 (2010)
- [25] O. Y. Tsupko and G. S. Bisnovaty-Kogan: *Gravit. Cosmol.* 18 117 (2012)
- [26] O. Y. Tsupko and G. S. Bisnovaty-Kogan, *Gravit. Cosmol.* 20 220 (2014)
- [27] V. Morozova, B. Ahmedov, A. Tursunov, *Astrophys. Space. Sci.* 346 513 (2013)
- [28] G. S. Bisnovaty-Kogan and O. Y. Tsupko: *Universe.* 3 1 (2017).
- [29] A. Abdujabbarov, B. Toshmatov, J. Schee, Z. Stuchlyk B. Ahmedov: *Int. J. Mod. Phys. D*26 1741011 (2017).
- [30] A. Abdujabbarov, B. Ahmedov, N. Dadhich, F. Atamurotov: *Phys. Rev. D*96 (2017) 084017.
- [31] C. A. Benavides-Gallego, A. A. Abdujabbarov, C. Bambi: *Eur. Phys. J. C*78 (2018) 694.
- [32] V. Perlick, O. Y. Tsupko, G. S. Bisnovaty-Kogan: *Phys. Rev. D*92 104031 (2015)
- [33] F. Atamurotov, B. Ahmedov and A. Abdujabbarov *Phys. Rev. D* 92 084005 (2015)
- [34] V. Perlick, O. Yu. Tsupko: *Phys. Rev. D* 95, 104003 (2017)
- [35] G. Z. Babarr, A. Z. Babar, F. Atamurotov: *Eur. Phys. J.* C80 761 (2020)
- [36] V. A. Kostelecky and S. Samuel: *Phys. Rev. Lett.* 63, 224 (1989)
- [37] V. A. Kostelecky and S. Samuel: *Phys. Rev. D* 39, 683 (1989);
- [38] V. A. Kostelecky and S. Samuel: *Phys. Rev. D* 40, 1886 (1989)
- [39] D. Colladay and V. A. Kostelecky, *Phys. Rev. D* 55, 6760 (1997).
- [40] D. Colladay, V.A. Kostelecky, *Phys. Rev. D* 55, 6760 (1997)
- [41] D. Colladay, V.A. Kostelecky, *Phys. Rev. D* 58, 116002 (1998)
- [42] V.A. Kostelecky, *Phys. Rev. D* 69, 105009 (2004)
- [43] S. K. Jha, A. Rahaman: Bumblebee gravity with a Kerr-Sen-like solution and its Shadow: arXiv:2011.14916
- [44] C. Ding, C. Liu, R. Casana, A. Cavalcante: *Eur. Phys. J. C*80, 178 (2020)
- [45] R. Casana, A. Cavalcante, F. P. Poulis, E. B. Santos: *Phys. Rev. D* 97, 104001 (2018)
- [46] Z. Li, A. Ovgun: *Phys. Rev. D* 101, 024040 (2020)
- [47] J. L. Synge *Relativity: The General Theory.* North-Holland, Amsterdam, 196
- [48] A. Abdujabbarov, B. Toshmatov, Z. Stuchlik and B. Ahmedov, arXiv:1512.05206
- [49] A. Rogers, *Mon. Not. Roy. Astron. Soc.* 451 17 (2015).
- [50] S. Dastan, R. Saffari, S. Soroushfar: arXiv:1610.09477
- [51] S. Hawking: *Commun. Math. Phys.* 43 199, (1975)
- [52] O. Y. Tsupko and G. S. Bisnovaty-Kogan, *Gravitation and Cosmology* 20, 220 (2014).
- [53] O. Y. Tsupko and G. S. Bisnovaty-Kogan, *Gravitation and Cosmology* 18, 117 (2012).
- [54] O. Y. Tsupko and G. S. Bisnovaty-Kogan, *Gravitation and Cosmology* 15, 184 (2009).
- [55] A. Abdujabbarov, B. Toshmatov, J. Schee, Z. Stuchlik, B. Ahmedov, *Int. J. Mod. Phys. D*26 1741011 (2017).
- [56] V. S. Morozova, B. J. Ahmedov, and A. A. Tursunov, *Astrophys. Space Sci.* 346, 513 (2013).